

## Short communication

## Effect of different oxides addition on the thermal expansion coefficients and residual stresses of Fe-based diamond composites

Ping Han<sup>a</sup>, Fu-ren Xiao<sup>a</sup>, Wen-jun Zou<sup>b</sup>, Bo Liao<sup>a,\*</sup><sup>a</sup>Key Lab of Metastable Materials Science & Technology and College of Material Science & Engineering, Yanshan University, Qinhuangdao 066004, China<sup>b</sup>College of Materials Science & Engineering, Henan University of Technology, Zhengzhou 450007, China

Received 8 July 2013; received in revised form 19 August 2013; accepted 19 August 2013

Available online 28 August 2013

## Abstract

CeO<sub>2</sub>, La<sub>2</sub>O<sub>3</sub>, Y<sub>2</sub>O<sub>3</sub>, and V<sub>2</sub>O<sub>5</sub> were added in an Fe-based matrix, and then the matrices were hot pressed at 700 °C. The thermal expansion coefficients and fracture stresses of the matrices were investigated, and residual stresses between the diamonds and matrices were simulated by finite element analysis. The weight losses of the specimens with diamonds were measured using a pin-on-disk wear testing rig. The surfaces from the wear tests were also examined by a scanning electron microscope. Results showed that the residual stress, difference of residual stress from fracture stress and weight loss all decreased after adding Y<sub>2</sub>O<sub>3</sub>, La<sub>2</sub>O<sub>3</sub>, V<sub>2</sub>O<sub>5</sub>, and CeO<sub>2</sub>, and the decrement increased in the same order. Among the four oxides, adding V<sub>2</sub>O<sub>5</sub> and CeO<sub>2</sub> remarkably improved the diamond retention capacity of the Fe-based matrix.

© 2013 Elsevier Ltd and Techna Group S.r.l. All rights reserved.

**Keywords:** Residual stress; Coefficient of thermal expansion; Diamond tool

## 1. Introduction

Given the extreme hardness of diamond, it is widely used as an abrasive element for polishing suspensions, as well as for grinding and cutting tools [1]. Four types of bonding systems, i.e., metallic, resinous, electroplated, and vitreous matrices, are used to fix diamond particles [2]. For metallic matrices, diamonds are mixed with metal powders, and the mixtures are sintered with powder metallurgy techniques. Hot pressing is widely used at present in fabricating diamond tools, and the pressure can activate sintering by inducing creep. The diamonds are bound by compression derived from shrinkage upon sintering, and the compressive stress arises from differences between the coefficients of thermal expansion (CTEs) of diamonds and metal matrix augmented by any volume change [3]. The thermal expansion mismatch between diamonds and metal matrix induces residual stress at the interface, which is responsible for retention capability [4]. A previous study has shown that the maximum tensile stress between the diamonds and elastic metal matrix is higher than the fracture stress of the

matrix, and cracks are easily generated at the interface. The diamond retention capacity of the matrix decreases, and diamonds are prematurely lost during the cutting action of a diamond tool [5]. Therefore, the decrease in mismatch between elastic metal matrix and diamonds can decrease residual stress and improve the retention capacity of the matrix.

The CTE of diamond is low at room temperature but sharply increases with increased temperature, e.g.,  $1.0042 \times 10^{-6}/^{\circ}\text{C}$  at 25 °C and  $4.9768 \times 10^{-6}/^{\circ}\text{C}$  at 1027 °C [6]. For metal matrices, a Co-based matrix has a similar thermal expansion characteristic that can result in good embedding and adherence between diamonds and matrix [7]. Therefore, cobalt powders are widely used to manufacture diamond tools [8]. However, Co is expensive because it is a strategic metal and a suspected carcinogen that necessitates stringent precautions during manufacture and use [9]. Considering all these negative points, numerous studies focus on Fe-based alloys with proper metals aiming at the substituent of the Co-based metal matrix, e.g., Fe–Cu–Co [10,11] and Fe–Ni [12] alloys. Ceramic particles such as SiC [13], CeO<sub>2</sub> [14], and La<sub>2</sub>O<sub>3</sub> [15] have been added into Fe-based alloy to improve its mechanical properties. In oxide dispersion-strengthened steels, adding Y<sub>2</sub>O<sub>3</sub> improves creep resistance at high temperatures after hot isostatic

\*Corresponding author. Tel./fax: +86 335 8077110.

E-mail addresses: [cyddjys@263.net](mailto:cyddjys@263.net), [frxiao@ysu.edu.cn](mailto:frxiao@ysu.edu.cn) (B. Liao).

pressing [16].  $V_2O_5$  is then added to bronze by spark plasma sintering [17].

In this work, Fe–Cu–Co–Ni–Sn alloys added with  $CeO_2$ ,  $La_2O_3$ ,  $Y_2O_3$ , and  $V_2O_5$  were prepared by hot pressing. The CTEs and fracture stresses of the five matrices with and without oxides were investigated. Residual stresses between the diamonds and matrices were simulated by finite element analysis (FEA). A computational strategy was developed to forecast the residual stresses between the diamonds and matrices with different thermal expansion properties.

## 2. Experimental procedure

### 2.1. Specimen fabrication and test methods

The starting metal materials used were  $<75\ \mu m$  Fe powder and electrolytic Cu powder, as well as  $<43\ \mu m$  Ni, Co, and Sn powders. The starting oxide materials used were  $10\ \mu m$   $CeO_2$  and  $La_2O_3$  powders, as well as  $5\ \mu m$   $V_2O_5$  and  $Y_2O_3$  powders. A mixture of Fe–30 wt.%Cu–10 wt.%Co–5 wt.%Ni–5 wt.%Sn composed the Fe-based matrix. 0.5 wt.%  $CeO_2$ ,  $La_2O_3$ ,  $Y_2O_3$ , and  $V_2O_5$  was added into the Fe-based matrix respectively. The five mixtures were blended for 2 h in a rotary mixer ( $\infty$ -shape), respectively. The mixtures were hot-pressed in graphite moulds for 2 min at  $700\ ^\circ C$  [18]. The specimens were rectangular and had dimensions of  $25\ mm \times 5\ mm \times 5\ mm$ .

CTEs were determined from  $700\ ^\circ C$  to room temperature ( $35\ ^\circ C$ ) using a high-precision thermal mechanical analyser (TMA) at a cooling rate of  $10\ ^\circ C\ min^{-1}$ . Data were collected in terms of linear change (LC) with respect to temperature. Fracture stress was measured by a three-point bending test. Diamonds of 170/200 US mesh were added in the five matrices, and the concentration of the diamonds was maintained at 25 vol%. The weight losses of the specimens with diamonds were measured using a pin-on-disk wear testing rig at a sliding speed of  $2.18\ m\ s^{-1}$  for 2 min, according to the method of Venkateswarlu [19]. This test was conducted against a 100 grit emery paper, and the applied load was 1.5 kg. The surfaces from the wear tests were also examined by a scanning electron microscope for microstructure evaluation.

### 2.2. Finite element modelling

FEA was performed to determine thermal residual stresses in each diamond particle after the cooling stage of the sintering process. Symmetric conditions were used for diamonds embedded in the five matrices. Three-dimensional shapes were modelled with two-dimensional axisymmetric elements, and ANSYS element Vector Quad 13 with eight nodes and reduced integration points was used. The diamond particles were assumed to be isotropic linear elastic with Young's modulus  $E=1050\ GPa$  and Poisson's ratio  $\nu=0.2$ . Simulation was performed using an elastic model that introduced the mechanical behaviour of the five matrices with Young's modulus  $E=185\ GPa$  and Poisson's ratio  $\nu=0.3$ . The CTEs of diamonds at different temperatures in Fig. 1 are taken from literature [6], and those of the five matrices were experimentally obtained.

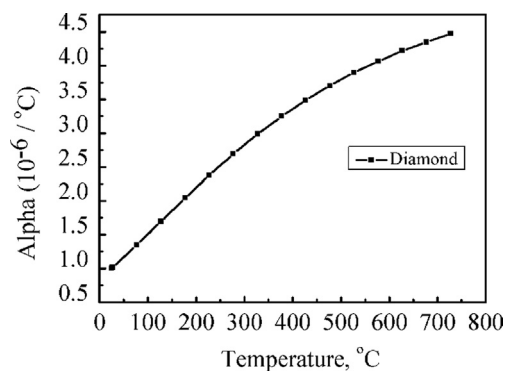


Fig. 1. The linear coefficient of thermal expansion (25–727 °C) of diamond.

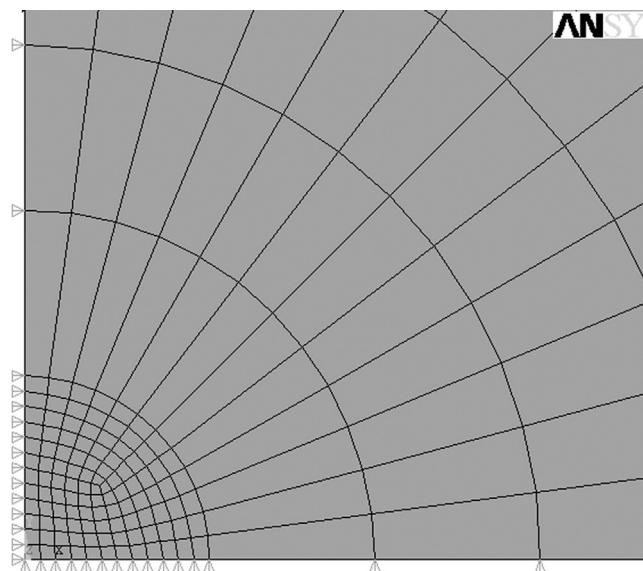


Fig. 2. Finite element model of the numerical analysis.

Fig. 2 presents the mesh used for numerical analysis. Only one quarter of the model was meshed because of symmetric conditions, in which a spherical diamond was surrounded by a spherical Fe-based matrix 10 times greater in size. A fine mesh was used close to the diamond for detailed investigation of residual stress. The nodes on the  $x$ -direction of the model were not allowed to move in the  $y$ -direction, and vice versa.

Zero stress of the diamond composites at the maximum hot pressing temperature was assumed. Thermal loads were applied under the assumption that temperature was spatially uniform throughout the composites. The composites were assumed to cool suddenly from the maximum hot pressing temperature to room temperature [20]. Therefore, no time-dependent stress relaxation during cooling was considered. FEA results were obtained, and the stress distribution fields around a diamond particle were visualised.

## 3. Results and discussion

### 3.1. Influence of different oxides addition on LC and CTE

The experimentally obtained LCs of the five matrices are shown in Fig. 3. The LCs of all matrices increase with

increased temperature, and the LCs of the matrices with oxides are higher than that of the matrix without oxide. The LC of the matrix with  $\text{CeO}_2$  is the lowest among the matrices with oxides, and the LCs of the matrices with  $\text{V}_2\text{O}_5$ ,  $\text{Y}_2\text{O}_3$ , and  $\text{La}_2\text{O}_3$  increase in the same order (Fig. 3b).

The CTEs of the matrices with  $\text{V}_2\text{O}_5$ ,  $\text{Y}_2\text{O}_3$ , and  $\text{La}_2\text{O}_3$  increase with increased temperature, as shown in Fig. 4. The CTEs of the three matrices increase in the same order as their LCs. The CTEs of the Fe-based matrix and the matrix with  $\text{CeO}_2$  increase with increased temperatures, except at 450 °C–650 °C.

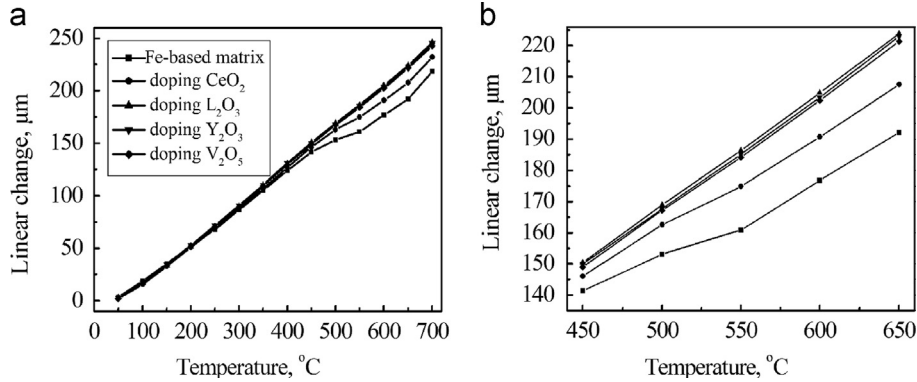


Fig. 3. Linear change of matrices versus temperature (a) 50–700 °C and (b) 450–650 °C.

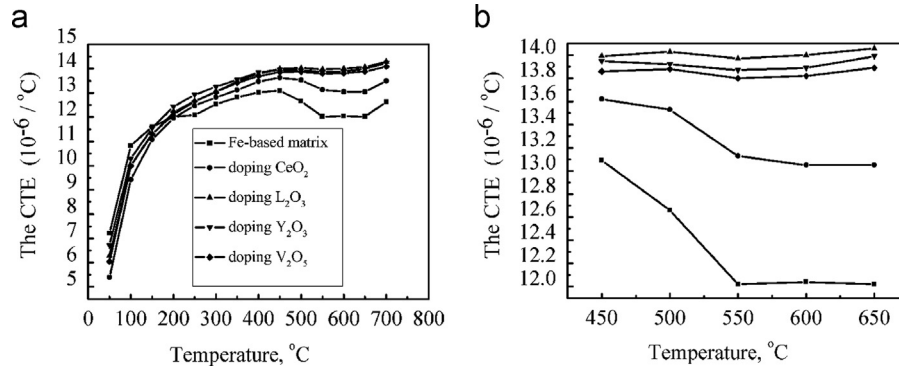


Fig. 4. The linear coefficient of thermal expansion of matrices versus temperature (a) 50–700 °C and (b) 450–650 °C.

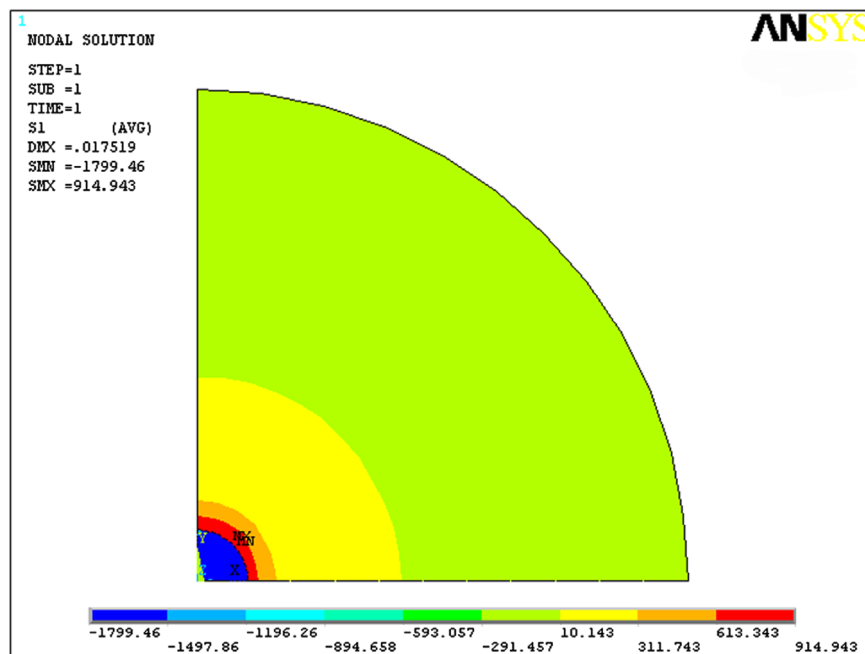


Fig. 5. Residual stress field around the diamond with the Fe-based matrix after hot-pressed at 700 °C.

Within this range, the CTE is an average value, and the increase rate of the LC is relatively low (Fig. 3). By contrast, the CTEs of the matrices with oxides are lower than that of the Fe-based matrix at  $< 100\text{ }^{\circ}\text{C}$  but higher at  $300\text{ }^{\circ}\text{C}$ – $700\text{ }^{\circ}\text{C}$ . These results indicate that adding oxides increases the thermal expansion mismatch between the diamonds and Fe-based matrix. The changes in CTE can be attributed to lattice distortion at the interface between the oxide and Fe-based matrix [21], which requires further investigation.

### 3.2. Influence of different oxides addition on residual stress field

The FEA results of the thermal stress fields of the five matrices are shown in Figs. 5–9. Two kinds of stress distribution exist after cooling, i.e., compressive and tensile stresses. Considering that the CTEs of the five matrices are larger than that of diamond, tensile and compressive stresses appear in the matrices and diamonds, respectively. Furthermore, the maximum tensile

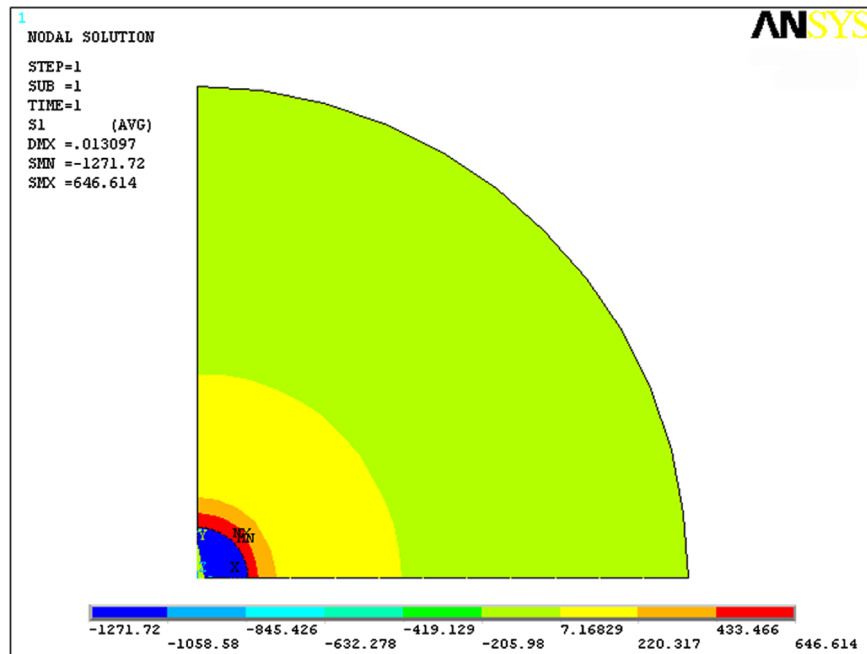


Fig. 6. Residual stress field around the diamond with the Fe-based matrix added  $\text{CeO}_2$  after hot-pressed at  $700\text{ }^{\circ}\text{C}$ .

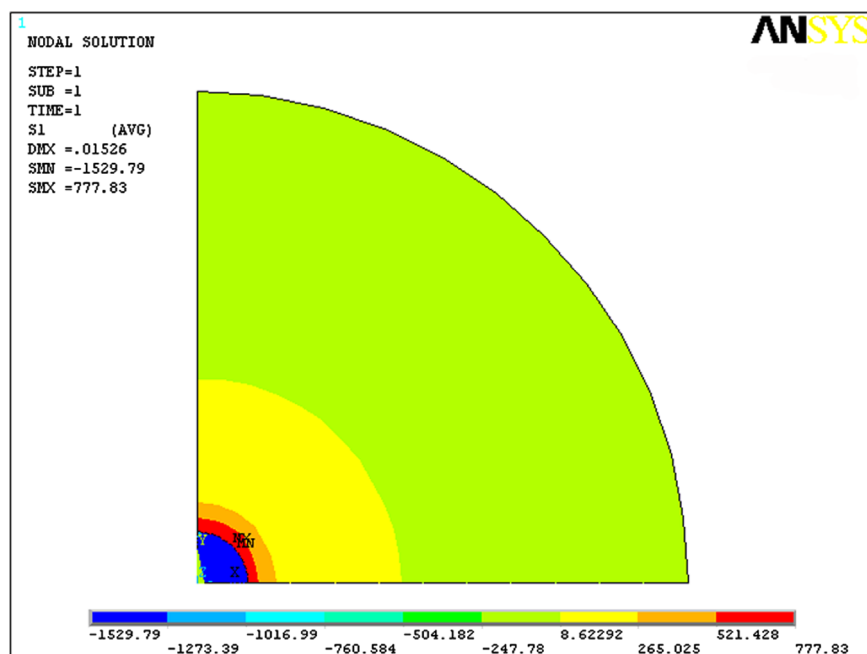


Fig. 7. Residual stress field around the diamond with the Fe-based matrix added  $\text{L}_2\text{O}_3$  after hot-pressed at  $700\text{ }^{\circ}\text{C}$ .

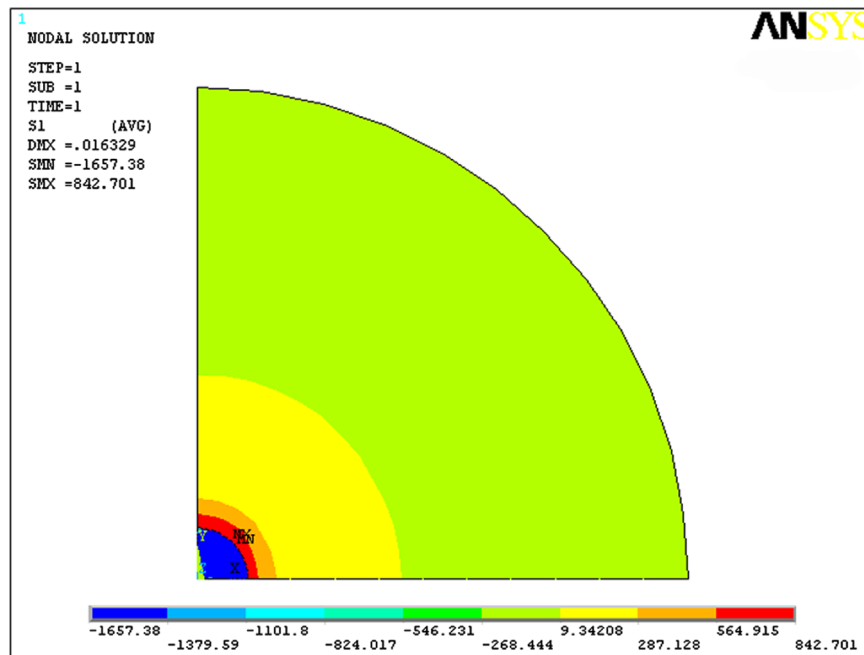


Fig. 8. Residual stress field around the diamond with the Fe-based matrix added  $Y_2O_3$  after hot-pressed at 700 °C.

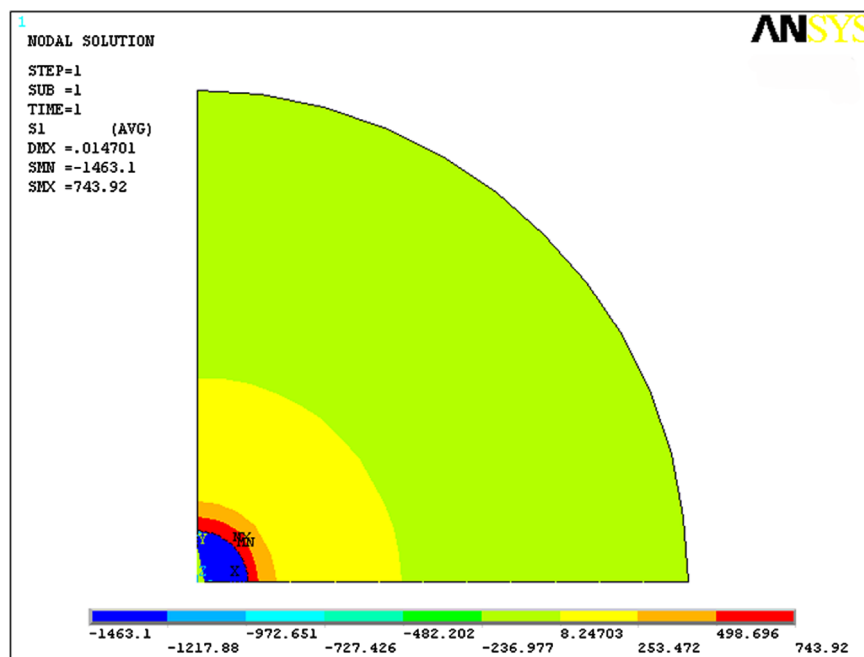


Fig. 9. Residual stress field around the diamond with the Fe-based matrix added  $V_2O_5$  after hot-pressed at 700 °C.

stress is located at the interface, and the tensile stress decreases away from the interface. Compressive stress is constant throughout the entirety of diamond particles.

The maximum tensile residual stress of the Fe-based matrix without oxide is around +914 MPa (Fig. 5), which is close to +970 MPa computed by procedures of ABAQUS in a previous research [5]. However, this residual stress is higher than the fracture stress (Table 1). Therefore, the interface is a potential site for crack initiation under thermal cycling, which

may lead to the occurrence of flaws and a decrease in the diamond retention capacity during the cutting action of a diamond tool. After adding  $CeO_2$ ,  $La_2O_3$ ,  $Y_2O_3$ , and  $V_2O_5$  in the Fe-based matrix, the maximum tensile residual stresses are about +646, +777, +842, and +743 MPa, as shown in Figs. 6–9, respectively. Compared with the Fe-based matrix, the maximum residual stresses of the matrices with oxides decrease by 29% ( $CeO_2$ ), 15% ( $La_2O_3$ ), 8% ( $Y_2O_3$ ), and 19% ( $V_2O_5$ ). The compressive stresses in the diamond particles



decrease with decreased tensile stress in the matrices. The residual stresses are quite inferior when ceramics are added, because they ease the stress state at the interface of metal matrix–diamonds.

Table 1 shows residual and fracture stresses, as well as their differences among the five matrices. The difference in the Fe-based matrix is the largest, i.e., 405 MPa, and the oxide additions decrease the differences. The differences among matrices follow the order  $Y_2O_3 > La_2O_3 > V_2O_5 > CeO_2$ . The differences in the matrices with  $V_2O_5$  and  $CeO_2$  reach 91 and 67 MPa, suggesting that adding  $V_2O_5$  and  $CeO_2$  remarkably improves the diamond retention capacity of the Fe-based matrix.

Fig. 10 shows the surfaces of the five matrices obtained by the wear test. Due to the occurrence of the large micro-cracking between the Fe-based matrix and diamond in Fig. 10a, its wear loss is the biggest among the five matrices in Fig. 11. As for the matrix with  $CeO_2$ , the contact between the diamond and matrix is the tightest in Fig. 10b, and its wear loss is the smallest among the five matrices. For the other three

matrices, the amount of the micro-cracking follow the order  $Y_2O_3 > La_2O_3 > V_2O_5$  in Fig. 10c–e, and the weight losses of the three matrices follow the same order in Fig. 11. The results of the weight loss and the microstructure after the wear test confirm the suggestion of improvement in diamonds' retention by adding oxides in the Fe-based matrix.

#### 4. Conclusions

The CTEs and residual stresses of Fe-based matrices with oxides were studied by experimental and FEA. Adding  $CeO_2$ ,  $La_2O_3$ ,  $Y_2O_3$ , and  $V_2O_5$  obviously affected the CTE and residual stress between the diamonds and matrices. The following conclusions were drawn.

- (1) The CTEs of matrices with  $V_2O_5$ ,  $Y_2O_3$ , and  $La_2O_3$  increased with increased temperature, and the CTEs of the three matrices increased in the same order. The CTEs of the Fe-based matrix and the matrix with  $CeO_2$  increased with increased temperature, except at 450 °C–650 °C.

Table 1  
Results residual and fracture stresses, as well as their differences among the five matrices.

Matrix	Residual stress (MPa)	Fracture stress (MPa)	Residual stress – fracture stress(MPa)
Fe-based matrix	914	509	405
Adding $CeO_2$	646	579	67
Adding $La_2O_3$	777	536	241
Adding $Y_2O_3$	842	513	329
Adding $V_2O_5$	743	652	91

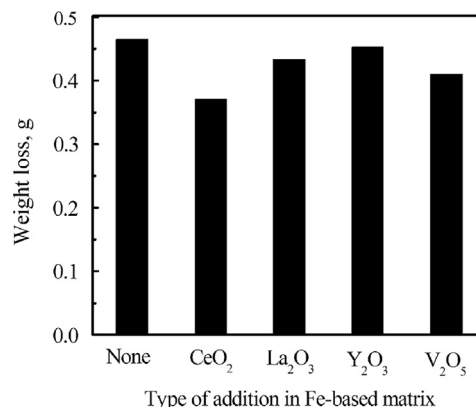


Fig. 11. Weight loss of different specimens after the wear tests.

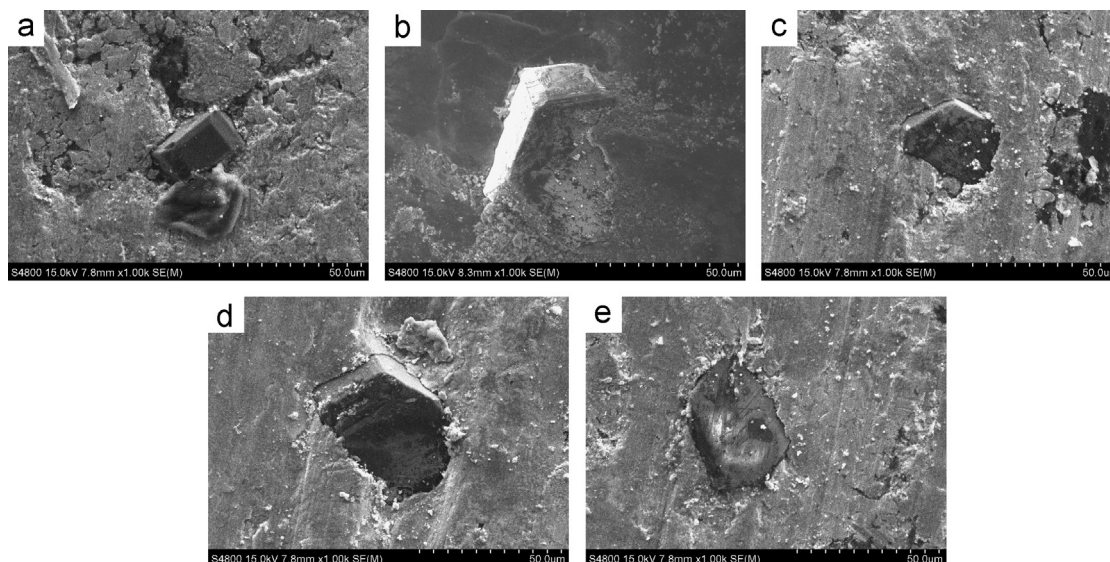


Fig. 10. Microstructures from the wear tests (a) Fe-based matrix, (b) Fe-based matrix added  $CeO_2$ , (c) Fe-based matrix added  $La_2O_3$ , (d) Fe-based matrix added  $Y_2O_3$  and (e) Fe-based matrix added  $V_2O_5$  respectively.

- (2) The residual stress, difference of residual stress from fracture stress and weight loss all decreased after adding  $\text{Y}_2\text{O}_3$ ,  $\text{La}_2\text{O}_3$ ,  $\text{V}_2\text{O}_5$ , and  $\text{CeO}_2$ , and the decrement increased in the same order.

Among the four oxides, adding  $\text{V}_2\text{O}_5$  and  $\text{CeO}_2$  remarkably improved the diamond retention capacity of the Fe-based matrix.

## References

- [1] C. Artini, M.L. Muolo, A. Passerone, Diamond–metal interfaces in cutting tools: a review, *Journal of Materials Science* 47 (2012) 3252–3264.
- [2] D. Herman, J. Krzos, Influence of vitrified bond structure on radial wear of cBN grinding wheels, *Journal of Materials Processing Technology* 209 (2009) 5377–5386.
- [3] S.W. Webb, Diamond retention in sintered cobalt bonds for stone cutting and drilling, *Diamond and Related Materials* 8 (1999) 2042–2052.
- [4] S. Spriano, Q. Chen, L. Settineri, S. Bugliosi, Low content and free cobalt matrices for diamond tools, *Wear* 259 (2005) 1190–1196.
- [5] B. Li, P.M. Amaral, L. Reis, C.A. Anjinho, L.G. Rosa, M. Freitas, 3D-modelling of the local plastic deformation and residual stresses of PM diamond–metal matrix composites, *Computational Materials Science* 47 (2010) 1023–1030.
- [6] R.R. Reeber, K. Wang, Thermal expansion, molar volume and specific heat of diamond from 0 to 3000 K, *Journal of Electronic Materials* 25 (1996) 64–66.
- [7] Q.H. Zou, H.M. Zhao, D.Y. Zhang, M. Geng, Z.G. Wang, J.J. Lu, Thermophysics characteristics and densification of powder metallurgy composite, *Powder Metallurgy* 49 (2006) 183–188.
- [8] J.D. Dwan, Impact properties of diamond impregnated metal matrices, *Industrial Diamond Review* 63 (2003) 50.
- [9] J. Konstanty, *Powder Metallurgy Diamond Tools*, Elsevier, Amsterdam, 2005.
- [10] A.P. Barbosa, G.S. Bobrovitchii, A.L.D. Skury, R.S. Guimarães, M. Filgueira, Structure, microstructure and mechanical properties of PM Fe–Cu–Co alloys, *Materials and Design* 31 (2010) 522–526.
- [11] G. Weber, C. Weiss, Diamix—a family of bonds based on diabase—V21, *Industrial Diamond Review* 2 (2005) 28–32.
- [12] Y.Z. Hsieh, S.T. Lin, Diamond tool bits with iron alloys as the binding matrices, *Materials Chemistry and Physics* 72 (2001) 121.
- [13] L.J. Oliveira, G.S. Bobrovitchii, M. Filgueira, Processing and characterization of impregnated diamond cutting tools using a ferrous metal matrix, *International Journal of Refractory Metals and Hard Materials* 25 (2007) 328.
- [14] Q.L. Dai, C.B. Luo, X.P. Xu, Y.C. Wang, Effects of rare earth and sintering temperature on the transverse rupture strength of Fe-based diamond composites, *Journal of Materials Processing Technology* 129 (2002) 427–430.
- [15] Y. Gao, Y.Q. Song, Z.J. Kang, Effects of lanthanum compounds on bonding in metal matrix–diamond composites, *Powder Metallurgy Industry* 11 (2001) 18–22 (In Chinese).
- [16] M. Klimiankou, R. Lindau, A. Möslang, HRTEM Study of yttrium oxide particles in ODS steels for fusion reactor application, *Journal of Crystal Growth* 249 (2003) 381–387.
- [17] J. Galy, M. Dolle, T. Hungria, P. Rozier, J.P. Monchoux, A new way to make solid state chemistry: Spark plasma synthesis of copper or silver vanadium oxide bronzes, *Solid State Sciences* 10 (2008) 976–981.
- [18] X.P. Xu, X.R. Tie, Y.Q. Yu, The effects of rare earth on the fracture properties of different metal–diamond composites, *Journal of Materials Processing Technology* 187–188 (2007) 421–424.
- [19] K. Venkateswarlu, A.K. Ray, M.K. Gunjan, D.P. Mondal, L.C. Pathak, Tribological wear behavior of diamond reinforced composite coating, *Materials Science and Engineering A* 418 (2006) 357–363.
- [20] K.P. Rao, D.P. Girish, M. Krishna, B.V. Madhu, Thermal mismatch stresses in a metal matrix composite—a finite element analysis, *International Journal of Advanced Engineering Technology* 1 (2011) 44–50.
- [21] Z.R. Xu, K.K. Chawla, R. Mitra, M.E. Fine, Effect of particle size on the thermal expansion of TiCAI XD™ composites, *Scripta Metallurgica et Materialia* 31 (1994) 1525–1530.